AD-A180 244 THE USE OF DEFORMATION MARKINGS TO ESTIMATE THE LAUNCH ACCELERATIONS EXPE..(U) MATERIALS RESEARCH LABS ASCOT VALE (AUSTRALIA) R WOODWARD ET AL. JAN 87 MRL-R-1039 1/1

UNCLASSIFIED F/G 19/1 NL

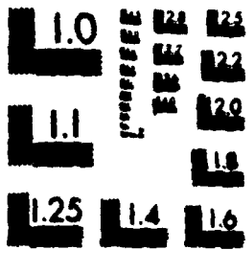

MICROCOPY RESOLUTION TEST CHART
NATIONAL BUREAU OF STANDARDS 1963 A

MRL-R-1039 AR-005-112

(12)

DEPARTMENT OF DEFENCE

DEFENCE SCIENCE AND TECHNOLOGY ORGANISATION

MATERIALS RESEARCH LABORATORIES

MELBOURNE, VICTORIA

REPORT

MRL-R-1039

THE USE OF DEFORMATION MARKINGS TO ESTIMATE THE LAUNCH ACCELERATIONS EXPERIENCED BY THE PHALANX ROUND

R. Woodward, B. Baxter, I.R. Johnston*, R.G. O'Donnell and S.D. Pattie

* Propulsion and Ballistics Division, Weapons System Research Laboratories, South Australia.

Approved for Public Release

JANUARY, 1987

DEPARTMENT OF DEFENCE
MATERIALS RESEARCH LABORATORIES

REPORT

MRL-R-1039

THE USE OF DEFORMATION MARKINGS TO ESTIMATE THE LAUNCH ACCELERATIONS EXPERIENCED BY THE PHALANX ROUND

R.L. Woodward, B.J. Baxter, I.R. Johnston*, R.G. O'Donnell and S.D. Pattie

ABSTRACT

Measurements were made on deformation marks in the pushers from launched Phalanx rounds and compared with similar marks from quasi-static tests to estimate the maximum force and torque between the penetrators and pusher at launch. It is demonstrated that these data can be combined with piezo-electric pressure data to make estimates of the maximum values of axial and circumferential accelerations, forces and circumferential torques. A more general application of the method to instrumentation of projectiles is discussed.

* Propulsion and Ballistics Division, Weapons Systems Research Laboratories, South Australia.

POSTAL ADDRESS: Director, Materials Research Laboratories
P.O. Box 50, Ascot Vale, Victoria 3032, Australia

AD-A180244

SECURITY CLASSIFICATION OF THIS PAGE **UNCLASSIFIED**

DOCUMENT CONTROL DATA SHEET

REPORT NO.	AR NO.	REPORT SECURITY CLASSIFICATION
MRL-R-1039	AR-005-112	Unclassified

TITLE

The use of deformation markings to estimate the launch accelerations experienced by the phalanx round

AUTHOR(S)
R. Woodward, B. Baxter,
I.R. Johnston, R.G. O'Donnell
and S.D. Pattie

CORPORATE AUTHOR
Materials Research Laboratories
P.O. Box 50,
Ascot Vale, Victoria 3032

REPORT DATE	TASK NO.	SPONSOR
January 1987	ODP 85/140	Office of Defence Production

FILE NO.	REFERENCES	PAGES
G6/4/8-3262	4	22

CLASSIFICATION/LIMITATION REVIEW DATE

CLASSIFICATION/RELEASE AUTHORITY
Superintendent, MRL
Metallurgy Division

SECONDARY DISTRIBUTION

Approved for Public Release

ANNOUNCEMENT

Announcement of this report is unlimited

KEYWORDS

Acceleration, Accelerometer's, Projectiles, Phalanx, Indentation

COSATI GROUPS 19040 14020

ABSTRACT

Measurements were made on deformation marks in the pushers from launched Phalanx rounds and compared with similar marks from quasi-static tests to estimate the maximum force and torque between the penetrators and pusher at launch. It is demonstrated that these data can be combined with piezo-electric pressure data to make estimates of the maximum values of axial and circumferential accelerations, forces and circumferential torques. A more general application of the method to instrumentation of projectiles is discussed.

CONTENTS

THE USE OF DEFORMATION MARKINGS TO ESTIMATE THE LAUNCH ACCELERATIONS EXPERIENCED BY THE PHALANX ROUND

1. INTRODUCTION

When a projectile is accelerated in a gun barrel it is subjected to external forces from the propellant combustion gases and interaction with the barrel, and to body forces which arise due to the acceleration and motion of the projectile. The forces result in stressing of the projectile components and for safe launch it is required that the stresses do not lead to fracture or gross yielding of the projectile. Various analytical, semi-empirical and finite element techniques have been used for launch stress evaluation, however there is a degree of uncertainty in the results because of the difficulty of obtaining experimental data during projectile launch. As maximum stresses are usually associated with maximum values of axial and angular acceleration or a combination of these, a method of determining values of these parameters would be useful. The present work outlines such a technique applied to the Phalanx projectile which is fired from the Vulcan gun system.

2. FORCES IN PROJECTILE ACCELERATION

Figure 1(a) and (b) show the external and the body forces respectively on a projectile during acceleration. The external forces include the pressure from the burning propellant and the interaction between the barrel and the projectile which occurs mainly through the driving band but involves some contact along the length of the projectile. The interaction force with the barrel can be resolved into a longitudinal retarding force and a tangential circumferential force which results in a torque and develops the spin in the projectile.

The body forces, Fig. 1(b), result from the axial acceleration and the angular acceleration and velocity. At a distance x from the base the axial force F_3 is required to accelerate the mass ahead of x. The angular

acceleration of the shell ahead of x results from a distribution of shear stress across the shell section at x. The resultant torque, τ_1, at that section can be equated to a circumferential force F_1 applied at the radius R of the shell. There is also a radial acceleration $\dot{\theta}$ due to the angular velocity, θ, of the projectile and this is balanced by a radial body force F_2 in the projectile and by the radial restraint of the gun barrel. The radial forces do not enter into the present study.

If the helix of the rifling is of angle, θ, then the angular acceleration $\dot{\theta}$ is related directly to the axial acceleration, a, by

$$\dot{\theta} = \left(\frac{a}{R}\right) \tan \theta \tag{1}$$

If the helix is of constant pitch then the maximum values of axial and angular acceleration occur at the same instant. However with a helix of variable pitch, as is the case with the Phalanx barrel, this is not necessarily so.

A photograph of the components of the Phalanx projectile is shown in Fig. 2. The projectile consists of a pusher which is acted on by the propellant gases and engages the rifling through a driving band, a sub-projectile and windshield (hereafter called the penetrator) which travel to the target, and a plastic sabot which separates when the projectile leaves the barrel. To transfer the rotation of the pusher to the penetrator, the design relies on the combined effects of the friction between the two components and axial inertia which enables the penetrator base to indent the pusher, as shown in Fig. 3, thus providing a mechanical coupling in rotation. For this analysis the penetrator and windshield were lumped together as one component. There is a strong mechanical joint between the sabot and the pusher so they too, are lumped together for the analysis of rotation forces. Further it was assumed that the interaction force between the barrel and the sabot was negligible compared with the interaction force between the pusher and the barrel.

A schematic diagram showing the arrangement of the components considered in this analysis is shown in Fig. 4(a). The axial forces on the base of the penetrator, F_p, the pusher, F_b, and the sabot F_s are related to the respective masses, m_p, m_b and m_s, through the axial acceleration, a, which is the same for each component,

$$F_p = m_p a \tag{2a}$$

$$F_s = m_s a \tag{2b}$$

$$F_b = F_p + F_s + m_b a + F_{bi} = P A_b \tag{2c}$$

or by re-expressing to emphasize the equation-of-motion aspect,

$$PA_b - F_{bi} = (m_b + m_p + m_s)a \tag{2d}$$

where F_{bi} is the axial component of the reaction force, F_R, between the rifling and the pusher. F_b is related to the area A_b of the base of the round and the pressure, P, at the base of the round due to the burning propellant gases. All the masses, the area A_b and the maximum pressure can be measured; thus a method of independently determining the maximum acceleration allows in turn the maximum values of all the forces between components to be obtained from equations (2).

Fig. 4(b) shows the torques, τ_p, between the pusher and the penetrator, and, τ_R, between the barrel and the pusher. The following relationships apply:

$$\tau_p = I_p \ddot{\theta} \tag{3a}$$

and

$$\tau_R - \tau_p = I_{b+s} \ddot{\theta} \tag{3b}$$

i.e.

$$\tau_R = (I_p + I_{b+s})\ddot{\theta}$$

where I_p is the moment of inertia of the penetrator,

I_{b+s} is the moment of inertia of the pusher and sabot lumped together, and

$\ddot{\theta}$ is the angular acceleration.

An independent determination of the maximum value of $\ddot{\theta}$ allows the maximum torques to be assessed. The effective circumferential force, F_c, at the driving band position required to provide τ_R is given by

$$F_c = \frac{\tau_R}{R} \tag{4}$$

In order to use equations (2) and (3) to evaluate the maximum forces and torques on the Phalanx round, a number of experimental values are required. By measuring the indentation of the penetrator into the pusher as a result of firing trials, and comparing this with quasi-static results, the force F_p between the projectile and the pusher can be estimated. Equation 2(a) then allows the maximum acceleration to be calculated. The peak gas pressure P can be measured by piezo-electric or copper crusher gauges. Equations (2) then allow all axial forces between components to be derived knowing the individual component masses and the area of the base of the round.

The torque τ_p between the penetrator and the pusher can similarly be deduced by comparing the torsional deformation in the pusher occurring during firing, with the deformation from quasi-static torsion tests. From a knowledge of the moments of inertia of the individual components, the maximum angular acceleration, maximum torque on the round, and the effective circumferential force can be found from equations (3) and (4).

The remainder of this report describes the measurement of the above parameters and their application to determine maximum values of force and torque for the Phalanx round.

3. EXPERIMENTAL METHODS

Figure 3 shows the slot at the base of a Phalanx round which is used to assist in transferring the spin from the pusher to the penetrator, and an example of the indentation in the pusher following firing of the round. Fig. 3(a) shows the penetrator base resting on the aluminium pusher before firing. In Fig. 3(b) the setback force during firing has enabled the penetrator base to indent into the pusher, thus filling the slot and producing a mechanical coupling. The torque produced in spin rotation partially shears the pusher material and the raised lips shown in Fig. 3(c) are due to this effect.

The pushers on which deformation markings were measured were collected from trials on an open range. In most cases copper crusher and piezo-electric peak pressure data were available for the firings. In addition, five projectiles were fired in an enclosed range to obtain pressure traces and maximum pressure data. In these latter tests the pusher was destroyed by impact with the target. Pressures were measured using a piezo-electric transducer located at the case mouth (where the projectile is crimped into the cartridge). These latter data give a good indication of the consistency of the firing parameters.

Masses of the components of the Phalanx round shown in Fig. 2 were determined by weighing. The moments of inertia about the cylindrical axis of the projectile, and of the pusher and sabot lumped together, were determined by measuring the period of oscillation of a torsion pendulum with the components attached as weights and comparing with simple cylinders machined from tungsten and perspex.

In order to determine the forces required to deform the pushers in the firings, the deformation needs to be reproduced under quasi-static conditions. Figure 5 shows schematically the arrangement used to quasi-statically load pushers in the laboratory, using a screw testing machine to apply the normal load and a lever to apply the torque. The loading rate is slow compared to the rates at launch in the gun, however errors due to strain rate effects on material properties, or to response rate of the system are expected to be small compared to the measured differences in deformation from round to round in the launched samples. A variety of axial loads was applied and the deformation measured using a Talylin machine. The comparison of this deformation with that on fired projectiles indicates the maximum load at launch. Using the appropriate normal load, a torque is then applied and the torque/time response recorded using a strain gauge transducer built into the subpress (Fig. 5). Deformation from the twisting was measured by the Talylin machine and also using a toolmaker's microscope to measure the total angle of twist.

4. RESULTS AND DISCUSSION

Table I lists the pressure data, from both copper crusher and piezo-electric gauges, the shear angle and the step height deformation data. Referring to Fig. 7(a) the step height is measured from the bottom of the indentation to the plateau made by the slot in the penetrator. The shear angle is the total angle of twist which is evident as a shear deformation of the step at two diagonally opposite corners in Fig. 3(c).

Figure 6 shows a typical pressure/time trace measured at the case mouth in the firings in the enclosed range using a service barrel. Peak pressure, muzzle velocity, ignition delay and action time for these firings are tabulated in Table II. The ignition delay is the time from application of the firing circuit EMF to the first rise in pressure as indicated on the pressure/time curve. The action time is the time from application of the firing circuit EMF to when the projectile exits the muzzle. The average pressure reading in Table II is lower than the average in Table I, because the trial data (Table I) were obtained by locating the transducer gauges to record the higher chamber pressures. The mean peak pressure from Table II was used for calculations as this is expected to represent the pressure on the base of the round at peak acceleration more accurately.

In the quasi-static tests, the heights of the step from the bottom of the indentation to the plateau and the heights of the shoulder from the step to the original surface were measured, Fig. 7(a). These data and the total indentation depth are tabulated in Table III as a function of load. The step height and total depth are plotted as a function of load in Fig. 7(b). The graph for step height tapers off in Fig. 7(b) because the slot used in the base for the quasi-static tests had the minimum depth of 0.18 mm. The range of step heights from the fired rounds is indicated in Fig. 7(b) and this gives an estimated range of the force F_p in equation 2(a) of 90 to 102 kN with a mean value of 96 kN (using the data of Table I).

In the quasi-static tests the torque was applied at four loading rates with a static indentation force of 80 kN. A typical torque/time curve is shown in Fig. 8. This shows that the torque rises to a peak at which yield occurs and then drops to a lower value as the projectile and pusher slip. Because the torque goes through a maximum, a measure of the total deformation does not indicate the torque reached. Table IV lists the results of the four tests showing the maximum and final torque, the total shear angle in the test and the rate of torque application. The mean maximum, τ_p in equation 3(a), is 38 Nm obtained as the mean of the peak torques in Table IV. The use of these data requires some interpretation and is discussed below.

The data of Table IV and the characteristic torque/time curve of Fig. 8 show that yielding in torsion occurs at some maximum torque and that further twisting to the final total shear angle occurs at some lower load. This is confirmed by Table I which shows quite a range of final shear angles from the fired pushers. These shear angles do not correlate in any way with the measured pressures. The use of this maximum torque value in equation 3(a) gives a maximum angular acceleration, $\dot{a}$, for the penetrator. Because slipping at a reduced load then occurs the maximum angular acceleration for the sabot

and pusher may be greater than this. Thus the resultant torque, τ_R, is underestimated using equation 3(b).

The masses and moments of inertia of the projectile components are listed in Table V. Using a mean pressure of 446 MPa and a projectile diameter of 20 mm, equations 2 to 4 may be solved to give the following typical quantities. The likely ranges for the parameters, based on the scatter of step heights in Table I and the range indicated in Fig. 7(b), are shown in brackets.

Maximum axial acceleration (a)	= 1.41×10^6 ms^{-2} (1.32-1.50)
Maximum axial force on Sabot (F_s)	= 12.2 kN (11.4-13.0)
Base driving force due to propellant gas (F_b)	= 140 kN (130-150)
Axial component of reaction force between pusher and barrel (F_{bi})	= 12.4 kN (20.5-4.4)
Maximum penetrator angular acceleration ($\dot{\omega}$)	= 3.54×10^7 rad s^{-2} (2.9-3.9)
Torque between barrel and pusher (τ_R)	= 83 Nm (68.5-91)
Circumferential force at driving band (F_c)	= 8.3 kN (6.8-9.1)

These data must be considered as representative only because of the variety of sources from which they were assembled. As indicated above, the torque between the barrel and the pusher, τ_R, and as a consequence also the circumferential force, F_c, are expected to be underestimated. The variation in step height and angle of shear in Table I must represent real variations in seating of the round and development of the twist during launch. The pressure data are quite consistent between shots and between the trial data Table I, and the shots fired in the enclosed range, Table II. There are insufficient data to assess whether a consistent trend exists between total indentation depth and total angle of shear at launch. For constant pitch rifling it is possible to use equation (1) with the above data to cross check the penetrator maximum axial and angular accelerations. However, in the present circumstance this is not possible because the Phalanx barrel has variable pitch rifling and the values of pitch (θ) at which the maximum angular and axial accelerations occur do not correspond.

The use of deformation to indicate maximum values of force has been used in the past, but required specially instrumented rounds to record the results. For instance, a survey of in-bore measurement methods (2), contains a reference (3) which describes a mass deforming a copper ball to indicate maximum force. Ball indentation gauges are also very reliable and well documented (4) and could have been used to determine maximum forces if the projectile itself did not already provide suitable data.

5. CONCLUSION

Examination of pushers recovered from Phalanx firings showed deformation markings caused by penetrator indentation and by the twisting due to spin. It was demonstrated by using information on the masses and moments of inertia of the projectile components, pressure measurements from the launch, and data on indentation forces and torques from quasi-static tests, that maximum values of launch acceleration forces and torques could be estimated. The values obtained are about 10% lower than those directly calculable using only the measured gas pressure and neglecting the effect of axial friction force in comparison with the force on the base of the projectile. The method thus provides a refinement of the values so obtained and provides a useful technique for measuring the axial force at shot start.

6. ACKNOWLEDGEMENT

The authors wish to acknowledge the assistance provided by Dr Ian Sach in the interpretation of the results.

7. REFERENCES

1. Lindeman, R.A., (1974). "Critical Evaluation and Stress Analysis of the 5"/54 HI-FRAG Projectile", NWL Tech. Rept. TR-3164, Naval Weapons Laboratory, Dahlgren, Virginia, July, 1974.

2. Sach, C.I. (1970), "In-Bore Ballistic Measurements a Survey of Techniques" TTCP Panel 0-6, Defence Standards Laboratory, Australia.

3. DeVost, V.F. (1960), "NOL Copper-ball accelerometers", Navord Report 6925, Nov. 1960.

4. Tabor, D. (1951), "The Hardness of Metals", Oxford, Clarenden Press.

TABLE I

Pressure and Impression Measurement Data from Trial Rounds

Round Indentification	T1	T4	T8	T11	T16	T18	T24
Copper Crusher Pressure (MPa)	396	390	385	396	374	385	-
Peak Piezo-electric Pressure (MPa)	454	451	451	-	464	463	-
Step Height (mm)	.153	.150	.198	.127	.157	.145	.178
Shear Angle	2.7^{o}	3.5^{o}	2^{o}	3.3^{o}	3.6^{o}	2.5^{o}	2^{o}

TABLE II

Firing Data from Enclosed Range Firings

Shot Number	Ignition Delay (ms)	Action Time (ms)	Peak Pressure (MPa)	Muzzle Velocity ms^{-1}
1	0.52	2.07	449.8	1155.4
2	0.55	2.11	435.3	1151.9
3	0.55	2.10	447.4	1154.5
4	0.57	2.12	441.1	1149.1
5	0.50	2.04	455.4	1159.8
Mean	0.54	2.09	445.8	1154.1

TABLE III

Quasi-Static Indentation Data

Load (kN)	Step Height* (mm)	Shoulder Height* (mm)	Indentation Depth* (mm)
60	.025	0	.025
70	.05	.005	.055
80	.08	.02	.10
90	.125	.05	.175
100	.152	.10	.252

* See Fig. 7(a) for definition.

TABLE IV

Results of Quasi-Static Torsion Tests*

Test No.	Shear Angle	Peak Torque (Nm)	Final Torque (Nm)	Torque Rate to Peak (Nms^{-1})
1	2.8	41.9	33	2.8
2	2.4	38	29	32
3	3.5	32	23	54
4	3.0	42	26	175

* Static indentation force of 80 kN.

TABLE V

Masses and Moments of Inertia of Projectile Components

Component	Mass (g)	Moment of Inertia (kg m^2)
Sabot	8.67)	1.261×10^{-6}
Pusher	13.72)	
Penetrator	68.05	1.089×10^{-6}

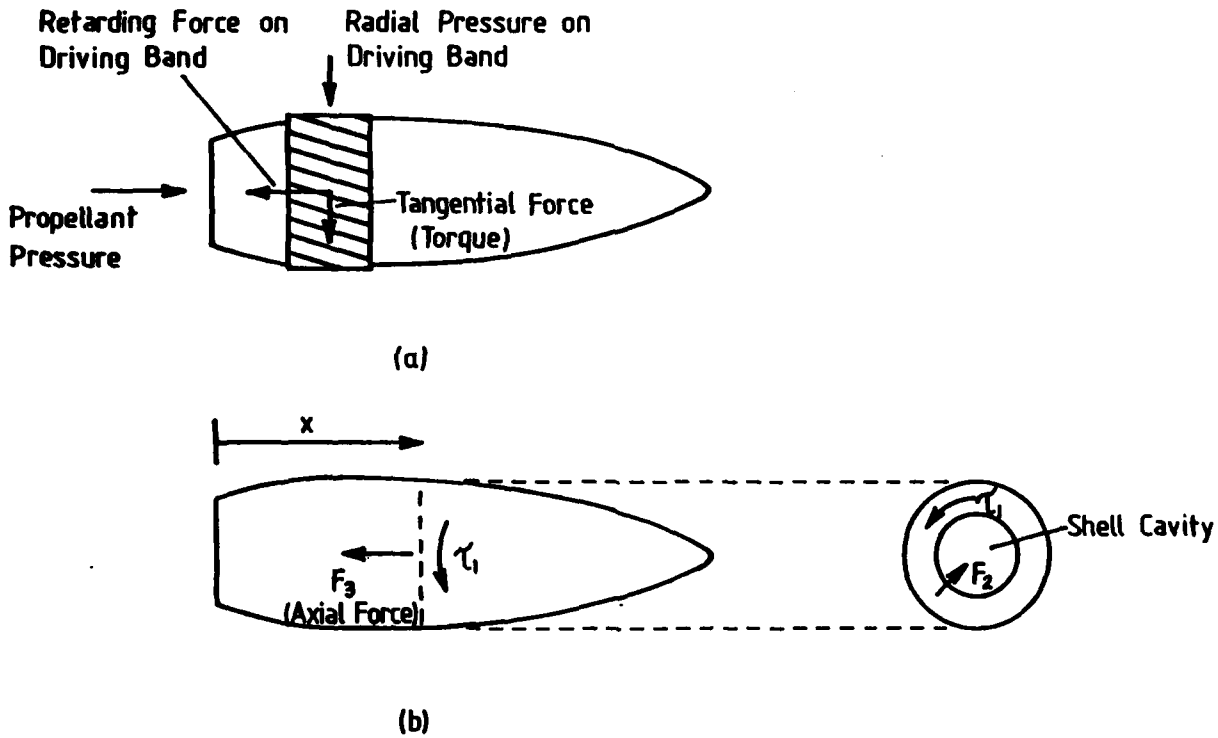

FIGURE 1 External and Body Forces acting on a projectile during firings.

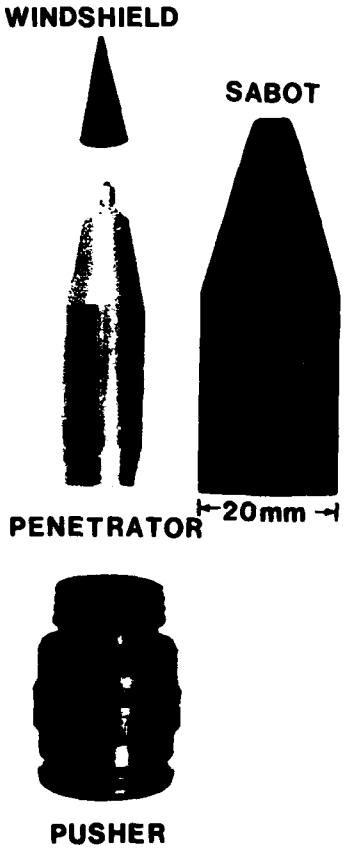

FIGURE 2 Phalanx Projectile Components.

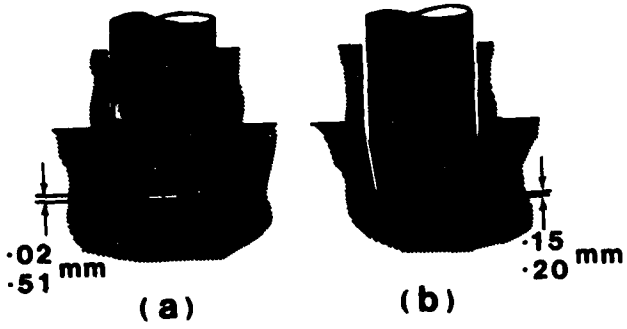

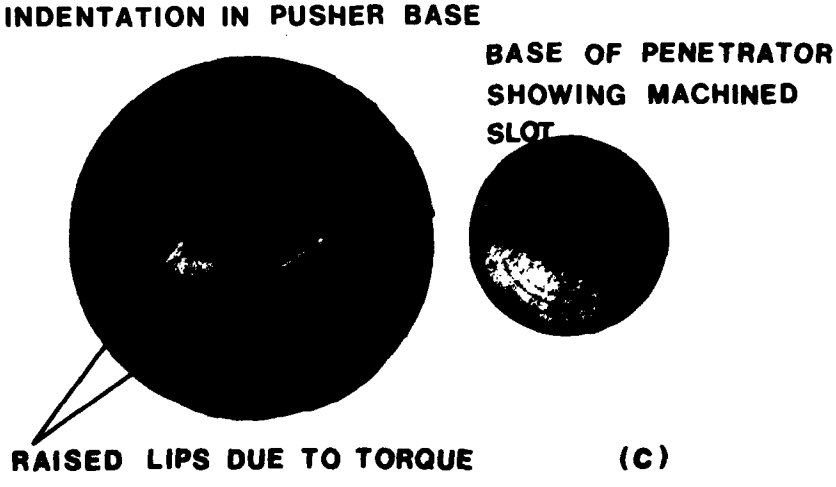

FIGURE 3 Projectile base and Pusher showing slot and indentation.

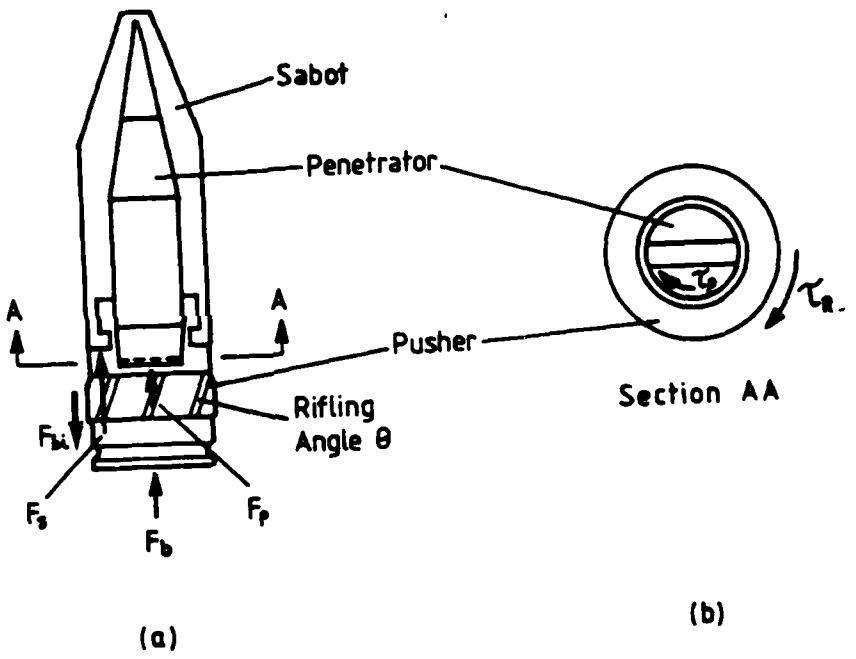

FIGURE 4 Schematic showing axial and rotational forces acting.

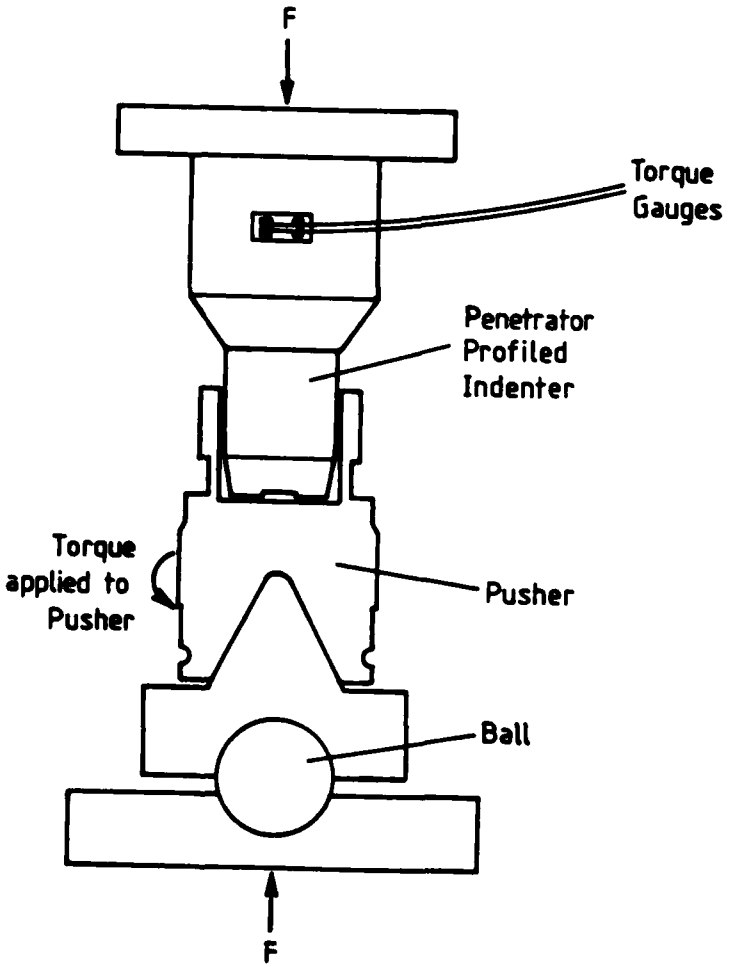

FIGURE 5 Apparatus for quasi static torque measurement.

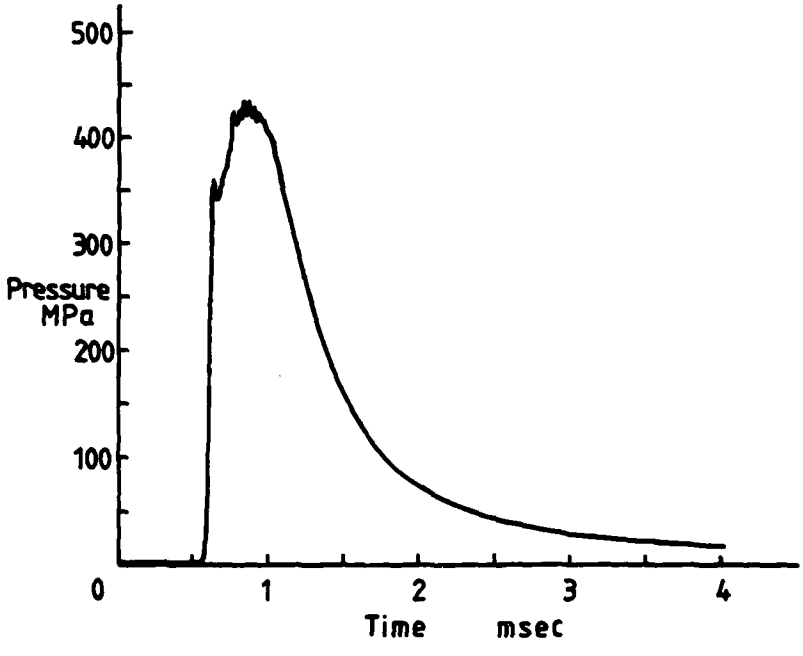

FIGURE 6 Pressure/time trace of Phalanx firing.

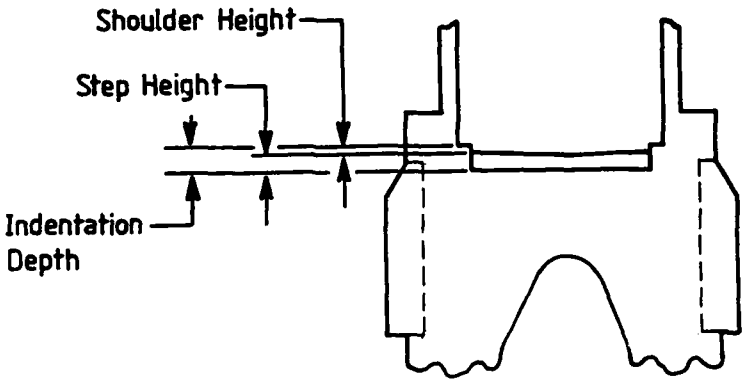

FIGURE 7a Illustration of step height on pusher.

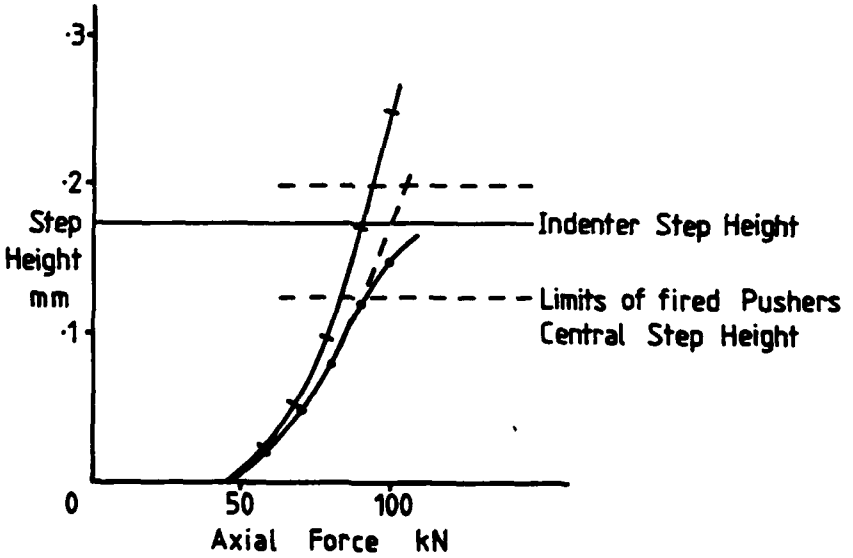

FIGURE 7b Load/indentation depth graph.

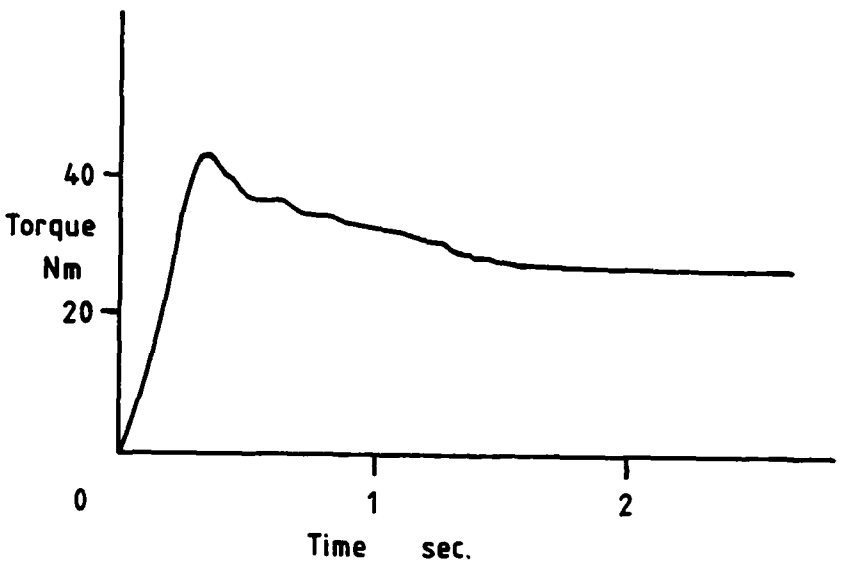

FIGURE 8 Quasi-static torque time plot.

END

DATE
FILMED

6-87